Improved photoconductive characteristics of solution-processed organic device by doping silole derivative

Ryohei Kobayashi[1], Takeshi Fukuda[1],Yuu Suzuki[1], Ken Hatano[1], Norihiko Kamata[1], Satoshi Aihara[2], Hokuto Seo[2], and Daiyo Terunuma[1]

[1] Department of Functional Materials Science, Saitama University

255 Shimo-Okubo, Sakura-ku, Saitama-shi, Saitama 338-8570, Japan

[2] NHK Science and Technical Research Laboratories

1-10-11 Kinuta, Setagaya, Tokyo 157-8510, Japan

Corresponding author: Takeshi Fukuda

Electronic mail: fukuda@fms.saitama-u.ac.jp

Tel and Fax: +81-48-858-3526

By doping 1,1-dimethyl-2,5-bis(N,N-dimethylaminophenyl)-3,4-diphenylsilole (silole-A) in poly(9,9-dioctylfluorene-alt-benzothiadiazole) (F8BT), an improved photoconductive characteristics was observed for a single layer organic device fabricated by a spin-coating process. A maximum external quantum efficiency (EQE) was 8.9 % at -20 MV/m when the ratio of silole-A:F8BT was 75 mol%. The EQE of the reference device with F8BT only was 0.06 %, and the highest EQE was approximately 160 times higher than that of the reference device. In addition, the photoluminescence (PL) quantum efficiency of the silole-A:F8BT neat film was lower than those of silole-A and F8BT neat films. The lower PL quantum efficiency indicates that the photo-induced carriers efficiently dislocate in the organic layer, resulting in the high EQE of organic photoconductive device.

Keyword: photoconductive device, color selectivity, solution process, polymer, silole derivative, image sensor

Introduction

In recent years, many organic devices have been attracting considerable attention due to a wide range of next generation printable electronics [1-4]. Most important advantages over inorganic devices are low fabrication cost using printing process and large substrate selectivity. In addition, several organic materials have singular spectral characteristics of the absorption spectrum at a visible wavelength region [5-7], and the particular high absorption coefficient leads us to realize color-selectable organic image sensor by stacking several organic layers with different absorption bands. Previous papers demonstrated the organic image sensor coupled to large area active matrix arrays [8] and the practical frequency response of organic photoconductive device for TV frame rate [9].

Since most of photo-excited carriers recombine in an organic layer without reaching electrodes as a photocurrent in the case of the single layer device, the single layer device has lower photoconductive characteristics than the multilayer device [7, 10]. The organic multilayer structure is difficult to fabricate by a conventional solution process,

however, the solution-processed organic photoconductive device has been necessary for the low fabrication cost and the large device area. Therefore, the carrier dislocation structure in the organic layer is important to cope with both low fabrication cost and high device performance. In the case of organic solar cells, the efficient carrier dislocation can be realized by using a bulk heterojunction structure with the mixture of poly(3hexylthiophene) and ([6,6]-phenyl C61-butyric acid methyl ester) [11-13]. However, little is known about the photoconductive characteristics of the color selective organic photoconductive device with a dopant to form the carrier pass to electrodes in the organic layer.

In this paper, we demonstrated the improved photoconductive characteristics of the blue-sensitive organic device fabricated by a conventional spin-coating process. We used poly(dioctylfluorenyl-co-benzo-thiadiazole (F8BT) as a photoconductive and blue-sensitive polymer and 1,1-dimethyl-2,5-bis(N,N-dimethylaminophenyl)-3,4-diphenylsilole (silole-A) as a carrier dislocation element in F8BT. Here,

F8BT has a suitable photoconductive polymer for the blue-sensitive device due to its high carrier mobility [14] and selective absorption spectrum at a blue wavelength region [7].

Experimental

At first, a glass substrate covered with a patterned indium tin oxide (ITO) was cleaned with organic solvents and deionized water under ultrasonic waves, and then treated with ultraviolet ozone for 20 minutes. The ITO layer with a thickness of 150 nm was deposited by a conventional sputtering method. A blue-sensitive organic photoconductive polymer of F8BT (American Dye Source, Inc.) was dissolved in chloroform as a content of 1 wt%. Then, silole-A was added in the resulting solution. The ratio of silole-A:F8BT was ranged from 0 to 200 mol% to investigate the concentration dependence on the photoconductive characteristics. Figure 1 shows molecular structures of F8BT and silole-A.

After passing through a filter with 0.45 μm holes, the organic solution was spin-coated at a rotation speed of 1000 rpm (above 50 mol%) and 1500 rpm (below 75 mol%) for 60 second in a nitrogen atmosphere. And then, the sample was annealed at 70 ℃ for 60 minutes in vacuum condition. Finally, LiF (0.1 nm) and Al (100 nm) were thermally evaporated successively on the top of a silole-A:F8BT layer.

The external quantum efficiency (EQE), defined as the number of output electrons divided by the total number of irradiated photons, was estimated from the measured photocurrent and the optical intensity of irradiated light. We used a blue light-emitting diode (LED) with center wavelengths of 470 nm, and the optical intensity was 2.5 mW/cm^2. The photocurrent was measured irradiating the blue light, and the dark current was also measured without irradiating the blue light.

In addition, the silole-A:F8BT neat film was spin-coated on a silica glass substrate. The ultraviolet-visible (UV-Vis) light absorption spectrum was recorded with a double-beam UV/Vis spectrophotometer (V-650, JASCO). The absorption coefficient was calculated from the transmittance and the thickness of the organic layer measured by a surface profile meter (Dektak3, ULVAC). In addition, The PL quantum efficiency

was measured by a luminance quantum yield measurement system (QEMS-2000, Systems Engineering Inc.), which consists of an integrated sphere and a UV LED with a center wavelength of 375 nm as an excitation source. The PL quantum efficiency was determined using a method based upon that originally developed by de Mello et al. [15]. In this approach, the quantum efficiency was given by the integrated PL intensity of the sample excited by the UV-LED divided by the decrease in the excitation intensity caused by inserting the sample into the integrated sphere.

Results and Discussion

Figure 2 shows the EQE of the organic photoconductive device as a function of the mol ratio of silole-A in F8BT. The electric field was calculated as the applied voltage divided by the thickness of silole:F8BT layer. The most important finding is that the EQE A increased up to the concentration of 75 mol%, and it decreased above 100 mol%. A maximum EQE of 8.9 % was achieved, and this value was approximately 160 times higher than that of the F8BT only device (0.06 %) at -20 MV/m. As clearly shown in Fig. 2,

the EQE at -20 MV/cm was higher than that at -10 MV/cm. This is because that the carrier mobility of organic materials increased with increasing the electric field [16], resulting in the efficient carrier dislocation in silole-A:F8BT layer.

The result can be explained on the basis of the energy diagram, as shown in Fig. 3. The highest occupied molecular orbital (HOMO) and lowest unoccupied molecular orbital (LUMO) energy level were determined by photoelectron spectroscopy and the absorption spectrum of neat film.

The HOMO and LUMO levels of silole-A was 5.19 and 2.75 eV, respectively. The HOMO level of silole-A was between those of ITO (4.80 eV) and F8BT (6.04 eV). Therefore, the photo-induced holes efficiently move to the ITO side when the negative bias voltage was applied to the ITO electrode. In addition, the LUMO level of silole-A was 2.75 eV, and the difference of LUMO level at the ITO/F8BT interface was 1.16 eV. Therefore, most of electrons inject to Al electrode without passing thought the LUMO level of silole-A. As a result, the efficient carrier dislocation can be realized in the silole-A:F8BT layer, and the EQE

was improved by doping silole-A in F8BT, as shown in Fig. 2.

Another possible reason of the improved EQE is the high carrier dislocation efficiency by doping silole-A in F8BT. This is because that the photo-induced electrons are pushed toward F8BT due to the low ionized potential of silole-A compared to that of F8BT. Therefore, the holes and electrons exit around silole-A and F8BT, respectively. The hypothesis can be explained by the PL quantum efficiency of the neat film, as shown in Fig. 4.

The PL quantum efficiency of the organic neat film without doping silole-A (F8BT only) was 40 %, and it rapidly decreased by doping silole-A. In addition, the PL quantum efficiency of silole-A neat film was 37 %, and it was higher than that of silole-A:F8BT. Furthermore, the minimum value of 2.4 % was observed at a mol ratio of 75 %. Therefore, the probability of photo-induced carrier recombination was reduced by mixing silole-A in F8BT. This is thought to be the reason for the decrease in the EQE. In addition, the dark current density decreased with increasing the concentration of silole-A. As a result, the EQE decreased with increasing the concentration of silole-A over 75 mol% owing to the low carrier transport efficiency.

Figure 5 shows the photocurrent and dark current of the organic photoconductive device with the silole-A:F8BT of 75 mol%. In both cases of photocurrent and dark current, a minimum current density was observed at an electric field of 5 MV/m. The photocurrent rapidly increased with decreasing the electric field less than 5 MV/m. However, the dark current was almost independent of the electric field when the negative bias voltage was applied to the device. Therefore, the signal-to-noise ratio, corresponding to the ratio between the photocurrent and the dark current, was improved with increasing the electric field. A maximum signal-to-noise ratio was 2170 at -20 MV/m, and it is high enough for practical applications.

The absorption spectrum of the silole-A:F8BT neat film is shown in Fig. 6. The inset of Fig. 6 indicates the relationship between the concentration of silole-A:F8BT and the maximum absorption coefficient at a wavelength range from 400 to 500 nm. The singular absorption spectrum was observed at a blue wavelength region, and it

decreased with increasing the concentration of silole-A. Both silole-A and F8BT have selective absorption at a blue wavelength region. The maximum absorption coefficient of the silole-A neat film was approximately 6000 cm^{-1} at the wavelength of 430 nm, and it was lower than that of F8BT. The fact indicates that the absorption coefficient of mixed film decreased with increasing the concentration of silole-A, as shown in the inset of Fig. 6. The transmittance of all the neat films at 470 nm was less than 15%, and it was high enough to absorb the incident light in the organic photoconductive layer.

These experimental results clearly indicate that a blue-sensitive organic photoconductive device has been achieved by using a conventional solution process, and the improvement in the photoconductive device was achieved by mixing silole-A and F8BT.

Conclusion

We have successfully achieved the improved EQE of a photoconductive device by adding silole-A in F8BT. A maximum EQE of 8.9 % was realized at a concentration of 75 % when the applied electric

field was -20 MV/m. The energy diagram and the low PL quantum efficiency indicate that the photo-induced carriers are easily dislocated in the soilole-A:F8BT layer. As a result, the carriers efficiently move to the electrode side with the low carrier recombination efficiency. In addition, his device showed the suitable photocurrent spectrum for the blue sensitive image sensor. These results indicate the possibility for the high performance organic image sensor by using a solution process.

References

[1] Tang, C.W., & VanSlyke, S.A., (1987). Appl. Phys. Lett., 51, 913.

[2] Sekitani, T., Noguchi, Y., Hata, K., Fukushima, T., Aida, T., & Someya, T., (2008). Science, 321, 1468.

[3] Shannon, J.M., & Balon, F., (2008). Solid State Electron., 52, 449.

[4] Wei, B., Kobayashi, N., Ichikawa, M., Koyama, T., Taniguchi, Y., & Fukuda, T., (2006). Opt. Exp., 14, 9436.

[5] Lamprecht, B., Thünauer, R., Köstler, S., Jakopic, G., Leising, G., & Krenn, J.R., (2008). Phys. Stat. Sol. (RRL). 2, 178.

[6] Aihara, S., Hirano, Y., Tajima, T., Tanioka, K., Abe, M., Saito, N., Kamata, N., & Terunuma, D., (2003). Appl. Phys, Lett., 82, 511.

[7] Fukuda, T., Komoriya, M. Kobayashi, R., Ishimaru, Y., & Kamata, N., (2009). Jpn. J. Appl. Phys., 47, 04C162.

[8] Street, R.A., Graham, J. Popovic, Z.D., Hor, A., Ready, S., & Ho, J., (2002). J. Non-Cry. Sol., 299-302, 1240.

[9] Fukuda, T., Komoriya, M., Mori, R., Honda, Z., Takahashi, K., & Kamata, N., (2009). Mol. Cryst. Liq. Cryst., 504, 212.

[10] Seo, H., Aihara, S., Watabe, T., Ohtake, H., Kubota, M., & Egami, N., (2007). Jpn. J. Appl. Phys., 46, L1240.

[11] Nelson, J., (2002). Org. Electron., 6, 87.

[12] Krebs, F.C., (2009). Sol. Ener. Mater. Sol. Cells, 93, 394.

[13] Pivrikaas, A., Sariciftci, N.S., Juška, G., & Österbacka, R., (2007). Prog. Photovolt: Res. Appl., 15, 677.

[14] Chua, L.-L., Zaumeil, J., Chang, J.-F., Ou, E. C. –W., Ho, P. K. –H., Sirringhaus, H., & Friend, R.H., (2005). Nature, 434, 194.

[15] Mello, J.C.de, Wittmann, H.F., & Friend, R.H., (1997). Adv. Mater. 9, 230.

[16] Matsushima, H., Naka, S., Okada, H., & Onnagawa, H., (2005). Curr. Appl. Phys., 5, 305.

Figure Captions

Fig. 1 Molecular structure of F8BT and silole-A used as the photoconductive layer.
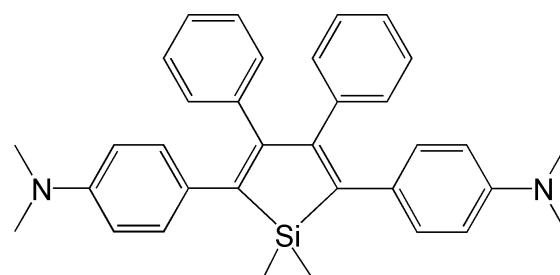
Fig. 2 Influence of the mol ratio of silole-A:F8BT on the EQE of the organic photoconductive device with difference applied electric fields. All the devices were excited by the blue LED with a center wavelength of 470 nm.

Fig. 3. Energy diagram of fabricated device with silole-A:F8BT as a photoconductive layer.
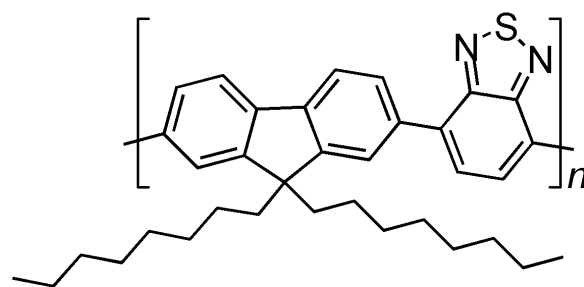
Fig. 4. Relationship between the PL quantum efficiency of silole-A:F8BT neat film and the mol ratio of silole-A:F8BT

Fig. 5 Photocurrent and dark current as a function of the electric field. The center wavelength and the intensity of irradiated light source were 470 nm and 2.5 mW/cm^2, respectively.

Fig. 6. Absorption spectrum of organic neat film. Inset shows the relationship between the concentration of silole-A:F8BT and the maximum absorption coefficient at a wavelength range from 400 to 500 nm.

Silole-A

F8BT

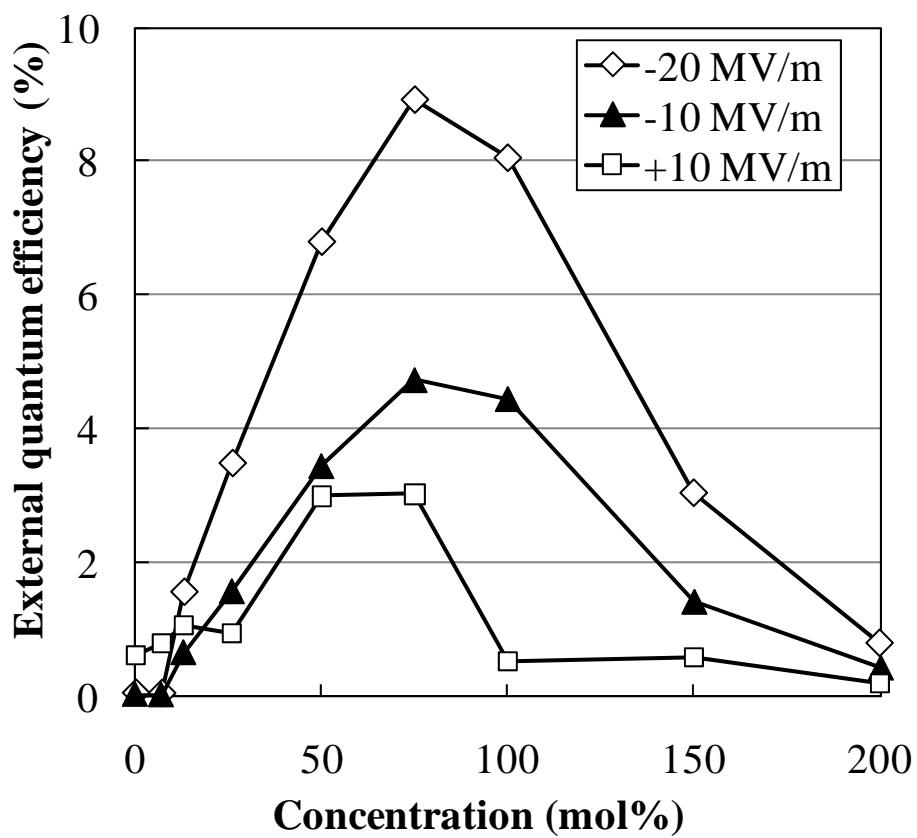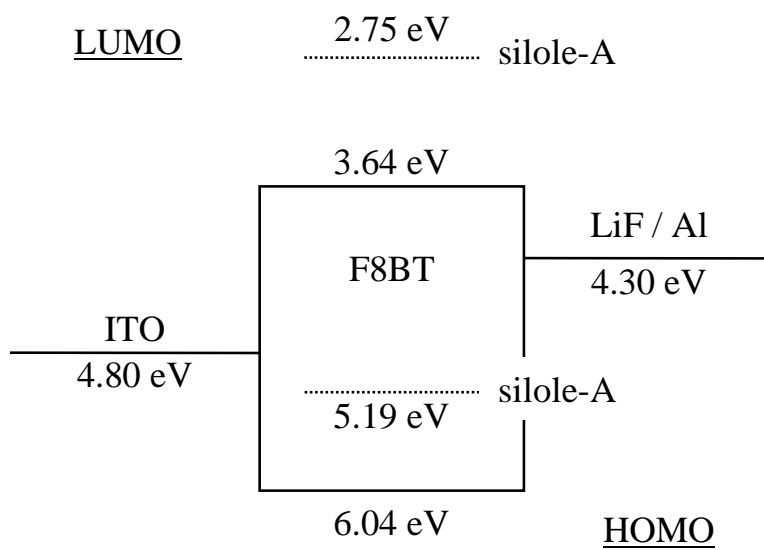Fig. 1. Molecular structure of F8BT and silole-A used as the photoconductive layer.

Fig. 2. Influence of the mol ratio of silole-A:F8BT on the EQE of the organic photoconductive device with difference applied electric fields. All the devices were excited by the blue LED with a center wavelength of 470 nm.

LUMO ___2.75 eV___ silole-A

3.64 eV

F8BT ____LiF / Al____
4.30 eV

ITO
4.80 eV _____ silole-A
5.19 eV

6.04 eV ___HOMO___

Fig. 3. Energy diagram of fabricated device with silole-A:F8BT as a photoconductive layer.

Fig. 4. Relationship between the PL quantum efficiency of silole-A:F8BT neat film and the mol ratio of
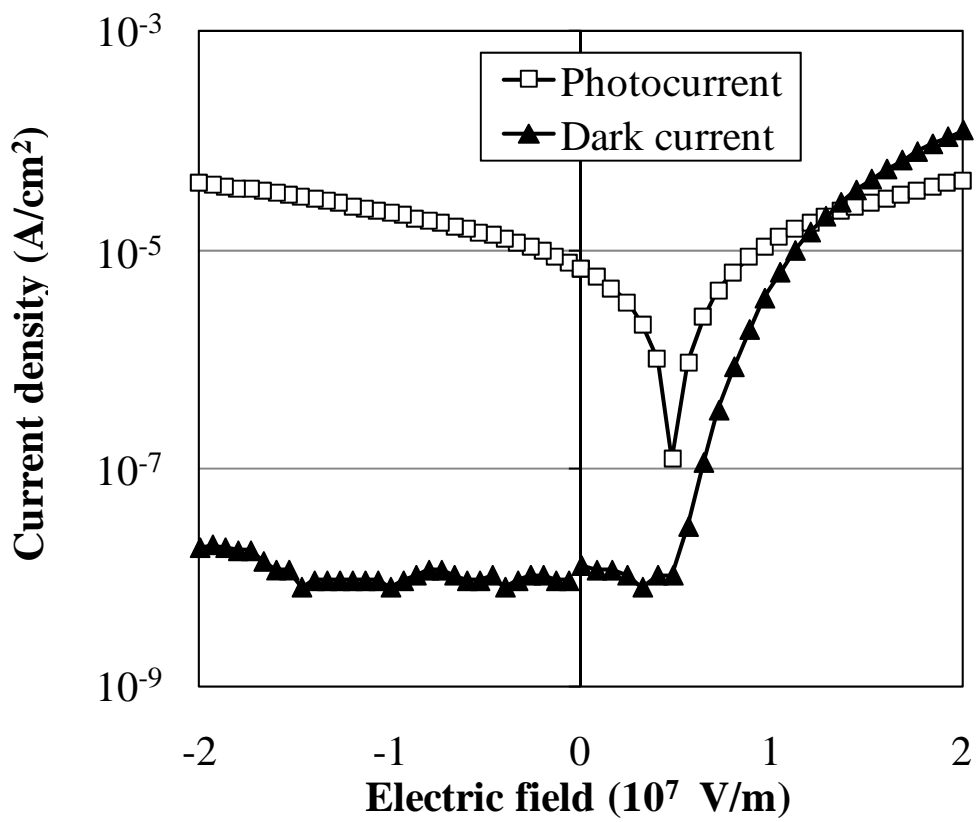
silole-A:F8BT

Fig. 5. Photocurrent and dark current as a function of the electric field. The center wavelength and the

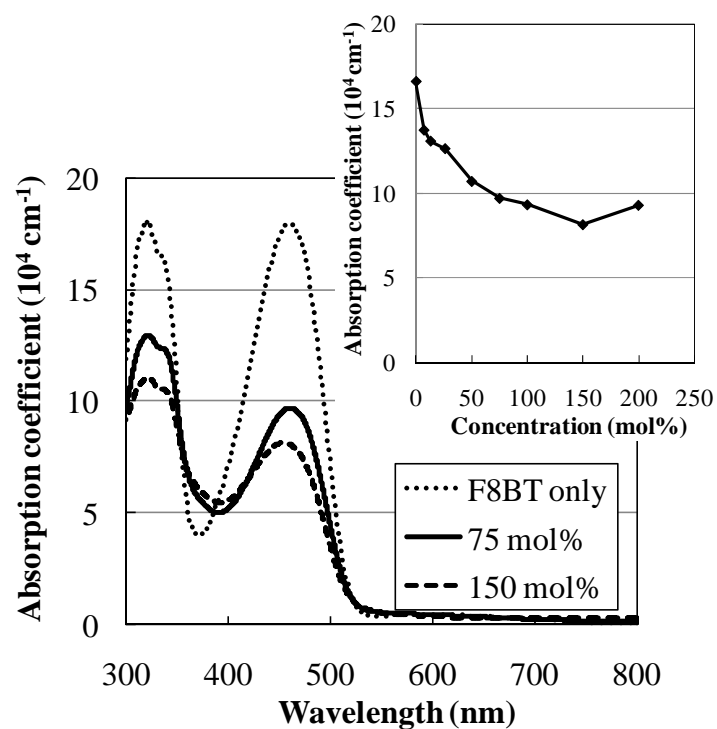intensity of irradiated light source were 470 nm and 2.5 mW/cm^2, respectively.

Fig. 6. Absorption spectrum of organic neat film. Inset shows the relationship between the concentration of silole-A:F8BT and the maximum absorption coefficient at a wavelength range from 400 to 500 nm.